

### Response to Referee 3

We sincerely thank the valuable comments and suggestions from Referee 3 and have extensively revised our manuscript accordingly. Here, we provide the point-by-point replies.

#### Referee 3

The manuscript introduces a relatively novel approach to enhancing the accuracy of  $m/z$  determination in single-particle mass spectra. While the authors claim a high calibration success rate of over 98%, it remains challenging to accurately assess the achieved accuracy.

The authors present several examples to demonstrate the precise identification of various ions. However, the arguments surrounding the separation of  $V^+$  and  $C_4H_3^+$  around  $m/z$  51, as well as the discussion on  $CaOH^+$  (56.95 Th) and  $C_3H_5O^+$  (57.05 Th), lack convincing evidence.

Regarding the separation of  $V^+$  and  $C_4H_3^+$ , the method suggests that they do not coexist within the same particles. However, there is a possibility that some peaks may have been misassigned. To clarify this, it would be beneficial to compare the presence of vanadium oxide ion ( $VO^+$ , 66.95 Th) in particles containing  $V^+$  and  $C_4H_3^+$ . Additionally, the random selection of only 10 particles may not be representative of the entire dataset. Given that over 100,000 mass spectra were obtained for these particles, a larger sample size should be considered for further analysis.

#### Response:

We thank Referee 3 for this suggestion and have added the required details. As shown in Figure 5b and 5c, in  $V^+$ -containing particles, the relative peak area of 66.95 Th peak is comparable to that of  $\sim 51$  Th peak. Instead, in  $C_4H_3^+$ -containing particles, no 66.95 Th peak could be observed, even in the logarithmic scale.

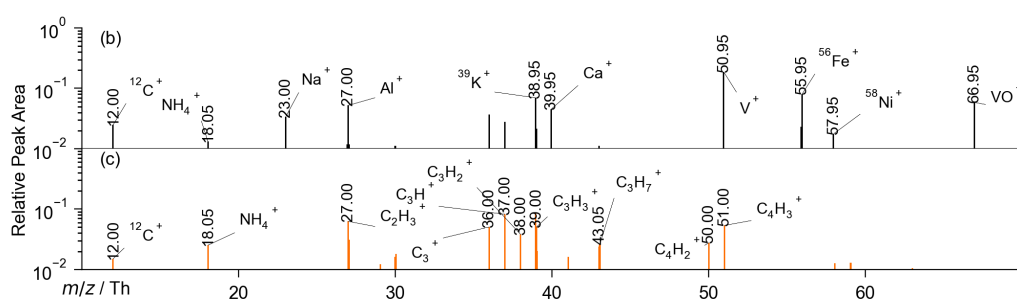


**Figure 5.** Averaged positive spectrum of (b)  $V^+$ -containing (in gray) and (c)  $C_4H_3^+$ -containing (in orange) particles were obtained by averaging millions of particles of the two particle groups separately.

To conduct a quantified comparison, we checked the average mass spectrum in terms of peak area (Figure S6). Again, there are strong 66.95 Th peaks in the  $V^+$ -containing particles, while in the  $C_4H_3^+$ -containing particles, we could not observe an evident 66.95 Th peak.

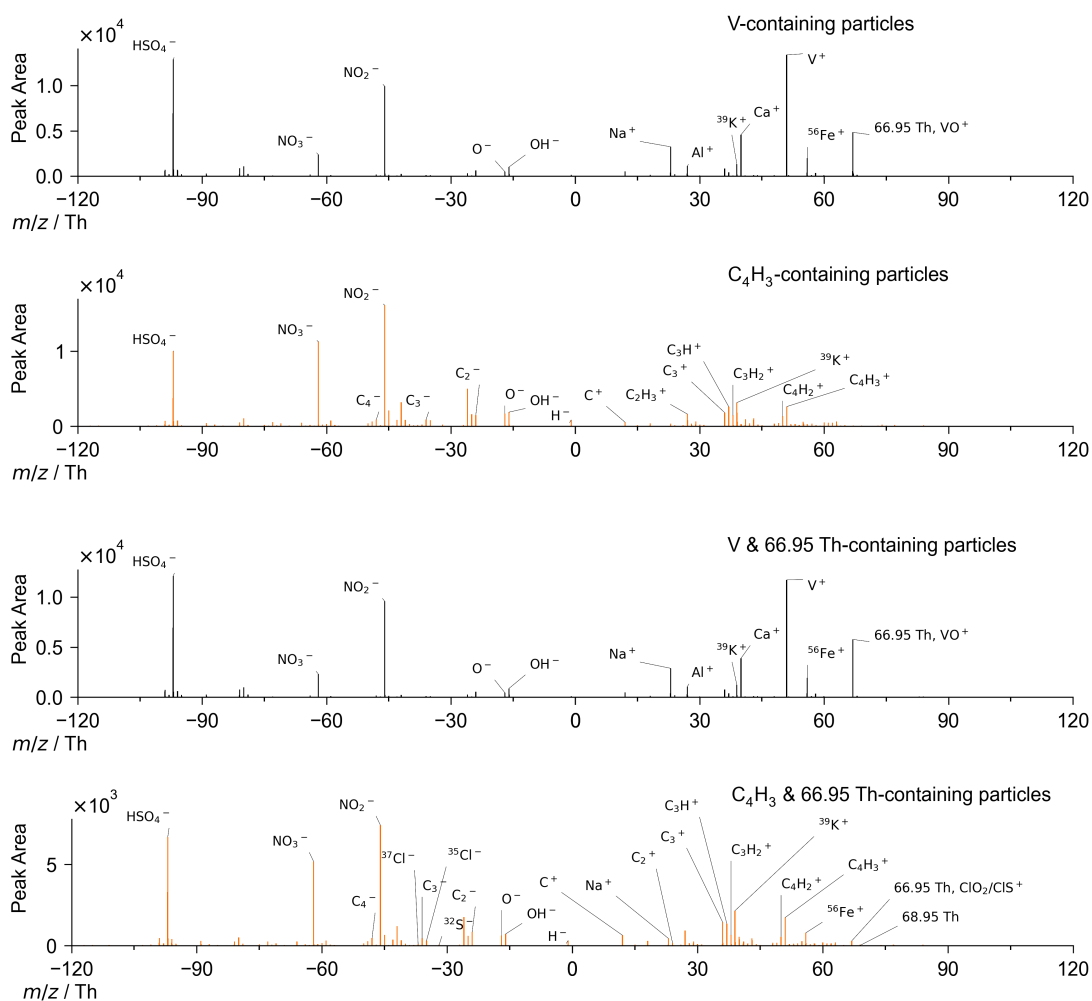


**Figure S6.** Averaged mass spectra of  $V^+$ -containing and  $C_4H_3^+$ -containing particles and  $V^+$ -containing and  $C_4H_3^+$ -containing particles that contain 66.95 Th signal. The average peak area of 66.95 Th in the  $V^+$  group is larger than 5,500, in the  $C_4H_3^+$  group the average peak area of 66.95 Th is  $\sim 300$  on average. The ratio of peak area of  $\sim 51$  Th peaks to 66.95 Th peaks in the two groups is 2.03 and 5.79, separately. The peak-area ratio of 66.95 Th : 68.95 Th in “ $C_4H_3$  & 66.95 Th” spectrum is 1 : 0.25 (300.10 : 72.40), the slight deviation from theoretical value (1 : 0.32) is likely due to the approaching of the signal-noise threshold (50), in the negative spectrum, the distribution of Cl<sup>-</sup> isotopes is  $-34.95$  Th :  $-36.95$  Th = 1 : 0.28 (306.92 : 87.32).

According to the averaged spectrum of “ $V^+$  & 66.95 Th” (Group 1) and “ $C_4H_3^+$  & 66.95 Th” (Group 2) (Figure S6), we can observe obvious differences in the chemical composition of these two particle groups. In the first group, metal signals are dominant. Further, at the single particle level, the fraction of 66.95 Th peak’s presence in  $V^+$  particles is 0.84, and the average peak area of 66.95 Th is larger than 5,500. However, in the second group, organic signals are dominant, especially the  $C_mH_n^+$  fragments from  $C_2H_3^+$  to  $C_4H_3^+$ , and the fraction of 66.95 Th peak’s presence is 0.15 (15,801 / 105,477) with average peak area around 300. In addition, the ratio of peak area of  $\sim 51$  Th to 66.95 Th in the two groups is quite different, i.e., 2.03 and 5.79, separately. In the ship-emitted particles similar to Group 1, previous studies reported that the intensity ratio of  $V^+ / VO^+$  is  $\sim 2$  (Anders et al., 2023; Zhai et al., 2023; Wang et al., 2019). From another perspective, in the mass spectrum of Group 2, we also observed a small peak at 68.95 Th that coexist with 66.95 Th. As the theoretical isotopic

distribution of  $\text{ClO}_2^+$  or  $\text{ClS}^+$  is  $66.95 \text{ Th} : 68.95 \text{ Th} = 1 : 0.32$ , we have observed a similar ratio as  $1 : 0.25$  ( $300.10 : 72.40$ ), the slight deviation from theoretical value is likely due to the approaching of the signal-noise threshold (50). In addition, in the negative spectrum, we could observe  $\text{S}^-$  and  $\text{Cl}^-$  isotopes. The theoretical distribution of  $\text{Cl}^-$  isotopes is  $-34.95 \text{ Th} : -36.95 \text{ Th} = 1 : 0.32$ , and we observe a close ratio  $1 : 0.28$  ( $306.92 : 87.32$ ). For these reasons, it seems the  $66.95 \text{ Th}$  peaks in the  $\text{C}_4\text{H}_3^+$ -containing particles should be assigned to  $\text{ClO}_2^+$  or  $\text{ClS}^+$ , whose  $m/z$  is also in the range of  $66.925\text{-}66.975 \text{ Th}$ . Therefore, we deduce that the misassignment rate of  $\text{V}^+$  and  $\text{C}_4\text{H}_3^+$  is restricted.

Additionally, we have modified our Figure 5e. The new Figure 5e involves 1000 randomly chosen particles from  $\text{V}^+$  and  $\text{C}_4\text{H}_3^+$  particles. The new figure is shown below:

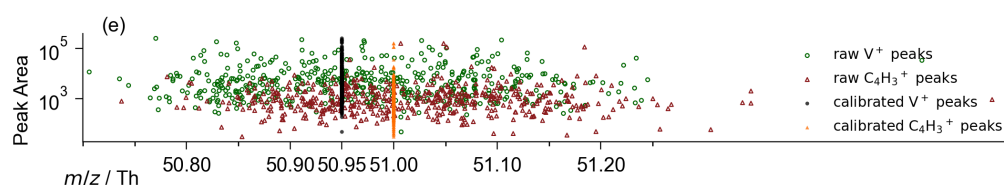


**Figure 5.** (e) Raw and calibrated peaks around 51 Th of 1000 randomly chosen  $\text{V}^+$ -containing or  $\text{C}_4\text{H}_3^+$ -containing particles

In general, according to the reasons above, we have modified our manuscript in Lines 229-255 as:

“The second pair is  $\text{V}^+$  (50.95 Th) and  $\text{C}_4\text{H}_3^+$  (51.00 Th).  $\text{V}^+$  is a typical marker of ship-emitted particles (Zhang et al., 2019a, b; Wang et al., 2019). Previously, the presence of  $\text{C}_4\text{H}_3^+$  often confuses the identification of  $\text{V}^+$  signals, because the mass difference ( $\sim 0.05 \text{ Th}$ ) is much less than the integer-level accuracy of the SPMS. Therefore, distinguishing  $\text{V}^+$  and  $\text{C}_4\text{H}_3^+$  in spectra is crucial in shipping aerosol research. By employing our standard-free calibration algorithm, the achieved high mass accuracy ensures the determination of  $\text{V}^+$  and  $\text{C}_4\text{H}_3^+$ . For instance, we randomly chose 10  $\text{V}^+$ -containing and 10  $\text{C}_4\text{H}_3^+$ -containing particles, with single-particle mass spectra (raw and calibrated) provided (Fig. S5). Further, we randomly chose 500  $\text{V}^+$ -containing and 500  $\text{C}_4\text{H}_3^+$ -containing particles to illustrate the calibration process. The peaks, both raw and calibrated, at  $\sim 51 \text{ Th}$  in these particles are illustrated in Fig. 5e, indicating that the corresponding species ( $\text{V}^+$  or  $\text{C}_4\text{H}_3^+$ ) of these peaks can easily be determined after our calibration (Fig. 5e, Text S4). Consequently, two distinct groups of mass spectra were isolated from our 12-million database of single-particle mass spectra, each containing 296,259 and 105,477 mass spectra with signals at 50.95 Th ( $\text{V}^+$ ) or 51.00 Th ( $\text{C}_4\text{H}_3^+$ ), respectively. The co-presence of  $\text{V}^+$  and  $\text{C}_4\text{H}_3^+$  signal in a single particle is theoretically permitted, though such a scenario was not observed in our database. In the mass spectrum of  $\text{V}^+$ -containing particles, the signal of vanadium oxide ion ( $\text{VO}^+$ , 66.95 Th), which is also a marker for shipping emissions, is present (Fig. 5b). Other ions of typical shipping emissions such as  $\text{Al}^+$  (27.00 Th),  $\text{K}^+$  (38.95 Th),  $\text{Ca}^+$  (39.95 Th),  $\text{Fe}^+$  (55.95 Th), and  $^{58}\text{Ni}^+$  (57.95 Th) are also detected (Zhang et al., 2019a). For the  $\text{C}_4\text{H}_3$ -containing group, signals of  $\text{C}_m\text{H}_n^+$  that correspond to organic aerosols could be observed (Fig. 5c). Further, the fraction of 66.95 Th peak’s presence in  $\text{V}^+$  and  $\text{C}_4\text{H}_3^+$  particles is 0.84 and 0.15, separately. The mass spectra of  $\text{V}^+$ -containing and  $\text{C}_4\text{H}_3^+$ -containing particles that contain 66.95 Th signal also have substantial differences in terms of both averaged peak area and the peak-area ratio of  $\sim 51 \text{ Th}$  peaks to 66.95 Th peaks (Figure S6). We also observed a peak at 68.95 Th that coexist with 66.95 Th in the 66.95 Th &  $\text{C}_4\text{H}_3^+$ -containing spectrum. Since the theoretical isotopic distribution of  $\text{ClO}_2^+$  or  $\text{ClS}^+$  is  $66.95 \text{ Th} : 68.95 \text{ Th} = 1 : 0.32$ , we have

observed a similar ratio in the mass spectrum as 66.95 Th : 68.95 Th = 1 : 0.25 (Figure S6). In addition, in the negative spectrum, we could observe S<sup>-</sup> and Cl<sup>-</sup> isotopes. The theoretical distribution of Cl<sup>-</sup> isotopes is -34.95 Th : -36.95 Th = 1 : 0.32, and we observed a close ratio 1 : 0.28. For these reasons, it is likely that 66.95 Th peaks in the C<sub>4</sub>H<sub>3</sub><sup>+</sup>-containing particles correspond to ions other than VO<sup>+</sup>, such as ClO<sub>2</sub><sup>+</sup> or ClS<sup>+</sup>, whose *m/z* is also in the range of 66.925-66.975 Th. Additionally, the time series of the two particle groups demonstrates distinct temporal behavior (Fig. 5d), in which the correlation coefficient between the two groups is ~0.15. The results confirmed our differentiation of previously confusing V<sup>+</sup>-containing or C<sub>4</sub>H<sub>3</sub><sup>+</sup>-containing particles. Moreover, the determination of adjacent ions also validates our calibration algorithm.”

Similarly, the discussion and validation surrounding the separation of CaOH<sup>+</sup> (56.95 Th) and C<sub>3</sub>H<sub>5</sub>O<sup>+</sup> (57.05 Th) are insufficient. It is anticipated that CaOH<sup>+</sup> (56.95 Th) peaks are more likely to coexist with Ca rather than C<sub>3</sub>H<sub>5</sub>O<sup>+</sup> (57.05 Th). A more detailed discussion on this relationship would help strengthen the argument.

**Response:**

We sincerely thank Referee 3 for the advice. We have checked the occurrence of C<sub>3</sub>H<sub>5</sub>O<sup>+</sup> and CaOH<sup>+</sup> in all Ca<sup>+</sup>-containing particles. We first isolated 910,483 Ca<sup>+</sup>-containing particles from our 12-million-particle dataset. The presence of CaOH<sup>+</sup> and C<sub>3</sub>H<sub>5</sub>O<sup>+</sup> in the Ca<sup>+</sup>-containing particles is listed below.

**Table S2.** The presence of ions in Ca<sup>+</sup>-containing particles.

Ion	Count	Fraction / %
Ca <sup>+</sup>	910,483	100
CaOH <sup>+</sup>	252,160	28
C <sub>3</sub> H <sub>5</sub> O <sup>+</sup>	79,155	8.7
CaOH <sup>+</sup> & C <sub>3</sub> H <sub>5</sub> O <sup>+</sup>	5,601	0.62

There are 28% of the Ca<sup>+</sup>-containing particles contain CaOH<sup>+</sup>, while the coexistence of Ca<sup>+</sup> and C<sub>3</sub>H<sub>5</sub>O<sup>+</sup> is limited to 8.7%. Further, particles containing both CaOH<sup>+</sup> and C<sub>3</sub>H<sub>5</sub>O<sup>+</sup> only constitute 0.62% of the Ca<sup>+</sup>-containing particles. Therefore, we consider Ca<sup>+</sup> & CaOH<sup>+</sup> & C<sub>3</sub>H<sub>5</sub>O<sup>+</sup>-containing particles as a rare subset of Ca<sup>+</sup>-containing particles. Further, we checked the mass spectrum of Ca<sup>+</sup>-containing, Ca<sup>+</sup> & CaOH<sup>+</sup>(only)-containing, Ca<sup>+</sup> & C<sub>3</sub>H<sub>5</sub>O<sup>+</sup> (only)-containing, and Ca<sup>+</sup> & CaOH<sup>+</sup> & C<sub>3</sub>H<sub>5</sub>O<sup>+</sup>-containing particles. The averaged mass spectra of these groups are provided as follows:

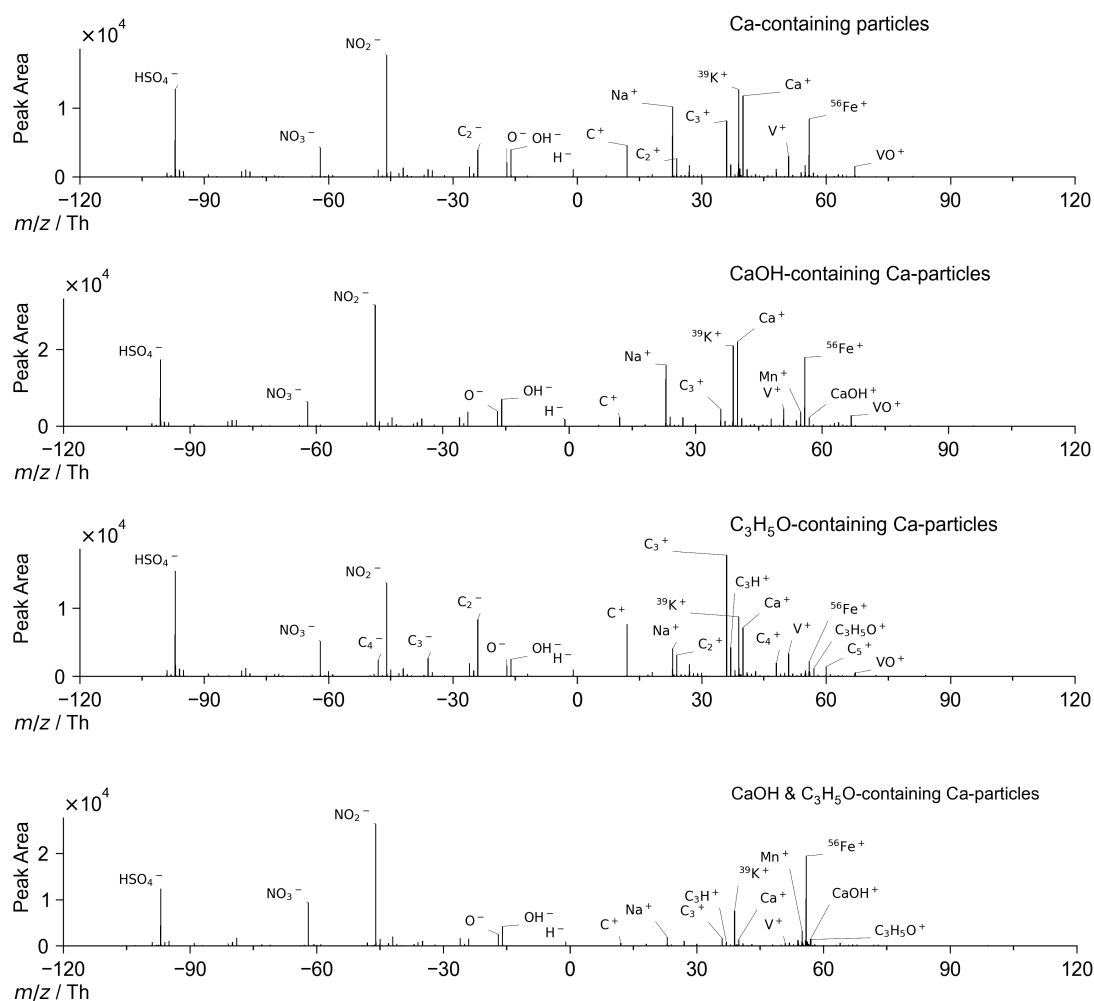


**Figure S4.** Averaged mass spectra of  $\text{Ca}^+$ -containing,  $\text{Ca}^+$  &  $\text{CaOH}^+$ (only)-containing,  $\text{Ca}^+$  &  $\text{C}_3\text{H}_5\text{O}^+$  (only)-containing, and  $\text{Ca}^+$  &  $\text{CaOH}^+$  &  $\text{C}_3\text{H}_5\text{O}^+$ -containing particles.

We find that  $\text{Ca}^+$  &  $\text{CaOH}^+$ (only)-containing particles have evident metal signals, while  $\text{Ca}^+$  &  $\text{C}_3\text{H}_5\text{O}^+$  (only)-containing particles have a series of organic fragments. Therefore, we anticipate that  $\text{Ca}^+$  &  $\text{CaOH}^+$  &  $\text{C}_3\text{H}_5\text{O}^+$ -containing particles contain both metal signals and organic fragments. The mass spectrum of  $\text{Ca}^+$  &  $\text{CaOH}^+$  &  $\text{C}_3\text{H}_5\text{O}^+$ -containing particles supports our expectation.

In general, we summarized the context above and modified the main text of our manuscript (Lines 221-228) as follows:

“The first pair is  $\text{CaOH}^+$  (56.95 Th) /  $\text{C}_3\text{H}_5\text{O}^+$  (57.05 Th). We isolated out 910,483  $\text{Ca}^+$ -containing particles from our 12-million dataset. In these particles, we mainly focused on the co-existence of  $\text{CaOH}^+$  and  $\text{C}_3\text{H}_5\text{O}^+$  in each spectrum. The searching criterion was *56.95 Th & 57.05 Th coexist in the individual spectrum*, and we have obtained 5,601 such spectra (Fig. 5a). The averaged mass spectrum of  $\text{Ca}^+$ -containing particles that contain only  $\text{CaOH}^+$  or  $\text{C}_3\text{H}_5\text{O}^+$  was also provided (Figure S4). In general, particles that contain both  $\text{CaOH}^+$  and  $\text{C}_3\text{H}_5\text{O}^+$  have characteristic signals of  $\text{CaOH}^+$ -containing and  $\text{C}_3\text{H}_5\text{O}^+$ -containing particles. It should be noted that the co-existence of  $\text{CaOH}^+$  and  $\text{C}_3\text{H}_5\text{O}^+$  is rare in the  $\text{Ca}^+$ -containing particles (Table S). Further, the co-existence of  $\text{CaOH}^+$  /  $\text{C}_3\text{H}_5\text{O}^+$  proved that adjacent peaks could be accurately

determined using our calibration algorithm, which means the information content of each spectrum is improved by our algorithm.”

## Reference

Anders, L., Schade, J., Rosewig, E. I., Kröger-Badge, T., Irsig, R., Jeong, S., Bendl, J., Saraji-Bozorgzad, M. R., Huang, J.-H., Zhang, F.-Y., Wang, C. C., Adam, T., Sklorz, M., Etzien, U., Buchholz, B., Czech, H., Streibel, T., Passig, J., and Zimmermann, R.: Detection of ship emissions from distillate fuel operation via single-particle profiling of polycyclic aromatic hydrocarbons, *Environ. Sci.: Atmos.*, 3, 1134–1144, <https://doi.org/10.1039/D3EA00056G>, 2023.

Wang, X., Shen, Y., Lin, Y., Pan, J., Zhang, Y., Louie, P. K. K., Li, M., and Fu, Q.: Atmospheric pollution from ships and its impact on local air quality at a port site in Shanghai, *Atmos. Chem. Phys.*, 19, 6315–6330, <https://doi.org/10.5194/acp-19-6315-2019>, 2019.

Zhai, J., Yu, G., Zhang, J., Shi, S., Yuan, Y., Jiang, S., Xing, C., Cai, B., Zeng, Y., Wang, Y., Zhang, A., Zhang, Y., Fu, T.-M., Zhu, L., Shen, H., Ye, J., Wang, C., Tao, S., Li, M., Zhang, Y., and Yang, X.: Impact of Ship Emissions on Air Quality in the Greater Bay Area in China under the Latest Global Marine Fuel Regulation, *Environ. Sci. Technol.*, 57, 12341–12350, <https://doi.org/10.1021/acs.est.3c03950>, 2023.